

Articles

Accessing Metal–Carbide Chemistry. A Computational Analysis of Thermodynamic Considerations

J. Brannon Gary, Corneliu Buda, Marc J. A. Johnson,* and Barry D. Dunietz*

Department of Chemistry, University of Michigan, 930 North University Avenue,
Ann Arbor, Michigan 48109-1055

Received March 6, 2007

The electronic structures of terminal metal carbide complexes are calculated using DFT. This study outlines the factors that give rise to stable carbide complexes, which can be used to help in the synthesis of new carbide complexes and to tune their stability as desired. The calculations reveal the presence of a strong Ru≡C triple ($\sigma + 2\pi$) bond. The C atom is nearly unhybridized, such that the C-component of the Ru–C σ -bond has 90% 2p character. This leaves a very stable carbon-based lone pair that is almost entirely 2s in character, which accounts for the lack of Lewis base character exhibited experimentally. Calculations predict a Ru–C bond dissociation energy of 147.4 kcal mol⁻¹ in a typical Ru carbide complex. This large bond strength is not unique to the Ru≡C bond, as revealed by an extension of the study to identify schemes by which to chemically tune the metal–carbide bond strength. Methods examined to achieve this tuning include changing the identity of the central metal and altering the metal ligation scheme. In general, 16-electron square-pyramidal M(C)L₄ complexes and 12- or 16-electron tetrahedral M(C)L₃ complexes of the 4d elements can possess comparably strong metal–carbide bonds. The calculations also show that the carbide moiety exerts a very strong trans influence, which explains several experimental observations. We conclude that the dearth of terminal carbide complexes is not due to any inherent weakness of M≡C bonds. Many more terminal carbide complexes can be expected in the future as new routes to their formation are found.

Introduction

Although terminal carbide complexes are very rare,^{1–7} they are of interest for several reasons. (Here we use the term “carbide” to denote the C₁ ligand without reference to the charge it carries. This parallels the common use of the term “hydride” to denote the H₁ ligand, regardless of the partial charge it carries. It also serves to highlight certain parallels to nitride ligands. The use of the term “carbon complex” has been proposed for a subset of carbide complexes in which the carbide ligand is a net donor to the metal, and thus has a small positive charge.⁸) In particular, neutral carbide complexes of ruthenium can serve as both decomposition products of and precursors to olefin metathesis catalysts. For example, decomposition of ruthenium-

based olefin metathesis catalysts can lead to inactive carbide-containing products.⁹ In the case of vinyl ester and vinyl carbonate substrates, we have shown that attempted cross-metathesis using Ru(CHPh)(PCy₃)₂Cl₂ (**Ru1E-CHPh**)¹⁰ and Ru(CHPh)(H₂IMes)(PCy₃)Cl₂ (**Ru3E-CHPh**)^{11–13} (H₂IMes = 4,5-dihydro-1,3-bis(mesityl)imidazol-2-ylidene) affords acyl-oxycarbene intermediates such as Ru(CHO₂CMe)(L)(PCy₃)₂Cl₂ (L = PCy₃, **Ru1E-CHOAc**; L = H₂IMes, **Ru3E-CHOAc**) that decompose quantitatively to the corresponding terminal carbide complexes Ru(C)(L)(PCy₃)Cl₂ (L = PCy₃, **Ru1E-C**; L = H₂IMes, **Ru3E-C**).^{7,14} Chart 1 depicts the complexes. The reaction mechanism underlying the spontaneous, irreversible **Ru1E-CHOAc** → **Ru1E-C** conversion has recently been studied computationally by DFT-based models, and two reasonable mechanisms have been identified.¹⁵ Very recently, we have noted that reactions of vinyl halides with **Ru3E-CHPh** can also

* Corresponding authors. Fax: (734) 647-4865. E-mail: mjaj@umich.edu.

(1) Peters, J. C.; Odom, A. L.; Cummins, C. C. *Chem. Commun.* **1997**, 1995.

(2) Greco, J. B.; Peters, J. C.; Baker, T. A.; Davis, W. M.; Cummins, C. C.; Wu, G. J. *Am. Chem. Soc.* **2001**, *123*, 5003.

(3) Enriquez, A. E.; White, P. S.; Templeton, J. L. *J. Am. Chem. Soc.* **2001**, *123*, 4992.

(4) Carlson, R. G.; Gile, M. A.; Heppert, J. A.; Mason, M. H.; Powell, D. R.; Vander Velde, D.; Vilain, J. M. *J. Am. Chem. Soc.* **2002**, *124*, 1580.

(5) Hejl, A.; Trnka, T. M.; Day, M. W.; Grubbs, R. H. *Chem. Commun.* **2002**, 2524.

(6) Romero, P. E.; Piers, W. E.; McDonald, R. *Angew. Chem., Int. Ed.* **2004**, *43*, 6161.

(7) Caskey, S. R.; Stewart, M. H.; Kivela, J. E.; Sootsman, J. R.; Johnson, M. J. A.; Kampf, J. W. *J. Am. Chem. Soc.* **2005**, *127*, 16750.

(8) Krapp, A.; Pandey, K. K.; Frenking, G. *J. Am. Chem. Soc.* **2007**, *129*, 7596.

(9) Hong, S. H.; Day, M. W.; Grubbs, R. H. *J. Am. Chem. Soc.* **2004**, *126*, 7414.

(10) Schwab, P.; Grubbs, R. H.; Ziller, J. W. *J. Am. Chem. Soc.* **1996**, *118*, 100.

(11) Scholl, M.; Ding, S.; Lee, C. W.; Grubbs, R. H. *Org. Lett.* **1999**, *1*, 953.

(12) Trnka, T. M.; Morgan, J. P.; Sanford, M. S.; Wilhelm, T. E.; Scholl, M.; Choi, T. L.; Ding, S.; Day, M. W.; Grubbs, R. H. *J. Am. Chem. Soc.* **2003**, *125*, 2546.

(13) Love, J. A.; Sanford, M. S.; Day, M. W.; Grubbs, R. H. *J. Am. Chem. Soc.* **2003**, *125*, 10103.

(14) Caskey, S. R.; Ahn, Y. J.; Johnson, M. J. A.; Kampf, J. W. submitted.

give rise to carbide complexes such as **Ru3E-C** via the intermediacy of the metathesis-active monohalomethylidene complexes $\text{Ru}(\text{CHX})(\text{H}_2\text{IMes})(\text{PCy}_3)\text{Cl}_2$ ($\text{X} = \text{F}, \text{Cl}, \text{Br}$).^{16,17} Thus, carbide formation appears to be one reason for the failure of cross-metathesis involving vinyl halides and several other α -heteroatom-substituted olefins. Conversely, Piers recently reported formation of olefin metathesis catalysts from **Ru1E-C** and **Ru3E-C**, upon protonation with strong acid.⁶

More generally, carbides are also implicated as key intermediates in the heterogeneous Fischer–Tropsch and related processes for catalytic formation of hydrocarbons and “oxygenates” (oxygen-containing compounds) from synthesis gas (CO/H_2),^{18–24} a proven method for converting coal into liquid fuels such as gasoline. The vast majority of carbido ligands bridge three or more metals in clusters. In these cases, their reactivity has been studied extensively, which has shown that encapsulation of the carbide ligand in metal clusters of nuclearity greater than four can lead to diminished reactivity.²⁵

In this study we focus on the surprising stability of **Ru1E-C** and **Ru3E-C**. These neutral carbides, unlike the first terminal carbido complex reported, anionic **Mo4E-C**,^{1,2} are only very weakly basic and nucleophilic and, in fact, do not react readily with air or water even in solution.^{4,5,7} Their activation can be achieved, however, when certain activated alkynes are added to form cyclopropenylidene complexes that can undergo further reactions to generate functionalized vinylidene complexes.²⁶ Lewis acid properties of **Ru1E-C** and **Ru3E-C** are even weaker than the Lewis base properties. Neither the Ru center nor the carbide ligand displays significant Lewis acid character in **Ru1E-C** and **Ru3E-C**. In addition, the ancillary ligands in **Ru1E-C** and **Ru3E-C** are much more inert toward substitution than are those in related carbene compounds (**Ru1E-CHPh**, **Ru1E-CHOAc**, **Ru3E-CHPh**, and **Ru3E-CHOAc** or their carbonyl and thiocarbonyl analogues **Ru1E-CO** and **Ru1-CS**) even though these molecules all have 16-electron counts at the Ru atom center and an approximate square-pyramidal coordination with the unique ligand in the apical position.^{4,5,7,10,13}

In the following sections we analyze the electronic structure of a range of carbide species, beginning with **Ru1M-C**, a model for the known complexes **Ru1E-C** and **Ru3E-C**. We investigate the bonding in terminal carbide complexes, including the effect of metal, ancillary ligands, and coordination geometry on the strength of the metal–carbide bond. We also examine the effect of substitution at the C atom to generate carbyne complexes. We highlight the geometries and electron counts that most favor strong metal–carbide bonds. We examine the trans influence of the carbide ligand and show how it influences the favored electronic structures and thereby determines which precursor complexes are the most suitable. Next, we show the origin of the surprising inertness of **Ru1E-C** and **Ru3M-C** to substitution

of the ancillary ligands. Finally, we examine the possibility of dimerization or ligand migration as likely decomposition processes. These new DFT calculations explain the surprising stability and inertness of **Ru1E-C** and its analogues.

Computational Details

All the carbene and carbide complexes are most stable in the singlet spin state except for **Ru7M-C**, which is a doublet, while the metal and ligand fragments possess various spin configurations. Geometry optimizations were followed by frequency calculations executed at several spin configurations to determine the ground state of each species. The calculations were carried out at the DFT level, employing the commonly used B3LYP functional^{27–29} and the LACVP* or LACVP** basis sets.³⁰ The Jaguar 6.5 package³¹ was used to implement the calculations. Coordinates for all atoms in the optimized structures are detailed in the Supporting Information. The bonding character between ligands and transition metals for several complexes are analyzed using natural bond orbital (NBO), and the orbitals were graphically plotted using Maestro.³² PCy_3 ligands are modeled by PMe_3 . Bond dissociation energy (BDE, ΔE) was calculated from the DFT energy difference between the optimized complex and optimized fragments. The corrected bond dissociation energy (BDE corr) accounts for the ZPE. Metal fragment reorganization energy ($\Delta E^*_{\text{reorg}}$) is calculated by the DFT energy difference of the metal fragment in its carbide geometry and optimized geometry. All ΔH and ΔG values are also corrected for zero-point energies.

Results and Discussion

Electronic Structure of $\text{Ru}(\text{C})(\text{PMe}_3)_2\text{Cl}_2$ (Ru1M-C**).** We consider **Ru1M-C** as the parent neutral carbide complex. The greater electronegativity of the C atom (relative to Ru) is expected to lead to energetically lower-lying atomic orbitals than the Ru atom's orbitals. Therefore, the bonding orbitals are expected to have greater contributions from C than from Ru. However, in all the Ru–C bonds of **Ru1M-C** we find larger orbital contributions from Ru than from C; that is, the bonds are polarized toward Ru. Furthermore, the calculated atomic charges (in **Ru1M-C**: Ru, -0.034 ; C, $+0.152$) indicate that C is a net donor ligand. However, the actual ligation scheme at the Ru atom and the sole participation of C 2p orbitals (i.e., the near-complete lack of C 2s orbital participation) in Ru–C bonding leads to the reversal of the anticipated ordering as indicated by NBO analysis³³ and illustrated in detail in Figure 1.

The NBO analysis of **Ru1M-C** indicates a Ru–C triple bond. There is one σ -bond between Ru ($4d_{z^2}$ atomic orbital with 62% contribution to molecular orbital) and C ($2p_z$, 38%) and two π -bonds: Ru ($4d_{yz}$, 78%)–C ($2p_y$, 22%) in the Cl–Ru–Cl plane (π_1) and Ru ($4d_{xz}$, 65%)–C ($2p_x$, 35%) situated in the P–Ru–P plane (π_2). The expected carbon-based lone pair of electrons occupies the nearly unhybridized C 2s orbital. These orbitals are depicted in Figure 1. The detailed NBO analysis is provided in Table S1 for **Ru1M-C** and the related carbene complexes **Ru1M-CH₂**, **Ru1M-CHPh**, and **Ru1M-CHOAc**.

The most stable spin configuration of the $\text{RuCl}_2(\text{PR}_3)_2$ fragment is highly dependent on the steric bulk of the PR_3

(15) Buda, C.; Caskey, S. R.; Johnson, M. J. A.; Dunietz, B. D. *Organometallics* **2006**, *25*, 4756.

(16) Macnaughtan, M. L.; Johnson, M. J. A.; Kampf, J. W. *Organometallics* **2007**, *26*, 780.

(17) Macnaughtan, M. L.; Johnson, M. J. A.; Kampf, J. W. *J. Am. Chem. Soc.* **2007**, *129*, 7708.

(18) Rofer-DePoorter, C. K. *Chem. Rev.* **1981**, *81*, 447.

(19) Snel, R. *Catal. Rev.-Sci. Eng.* **1987**, *29*, 361.

(20) Vanderlee, G.; Ponc, V. *Catal. Rev.-Sci. Eng.* **1987**, *29*, 183.

(21) Wojciechowski, B. W. *Catal. Rev.-Sci. Eng.* **1988**, *30*, 629.

(22) Forzatti, P.; Tronconi, E.; Pasquon, I. *Catal. Rev.-Sci. Eng.* **1991**, *33*, 109.

(23) Roberts, M. W. *Chem. Soc. Rev.* **1977**, *6*, 373.

(24) Sung, S. S.; Hoffmann, R. *J. Am. Chem. Soc.* **1985**, *107*, 578.

(25) Shriver, D. F.; Sailor, M. J. *Acc. Chem. Res.* **1988**, *21*, 374.

(26) Caskey, S. R.; Stewart, M. H.; Johnson, M. J. A.; Kampf, J. W. *Angew. Chem., Int. Ed.* **2006**, *45*, 7422.

(27) Becke, A. D. *J. Chem. Phys.* **1993**, *98*, 5648.

(28) Vosko, S. H.; Wilk, L.; Nusair, M. *Can. J. Phys.* **1980**, *58*, 1200.

(29) Lee, C. T.; Yang, W. T.; Parr, R. G. *Phys. Rev. B* **1988**, *37*, 785.

(30) Hay, P. J.; Wadt, W. R. *J. Chem. Phys.* **1985**, *82*, 299.

(31) *Jaguar 6.5*; Schrodinger L.L.C.: New York, 2005.

(32) *Maestro 6.5*, Schrodinger L.L.C.: Portland, OR, 2004.

(33) See Supporting Information.

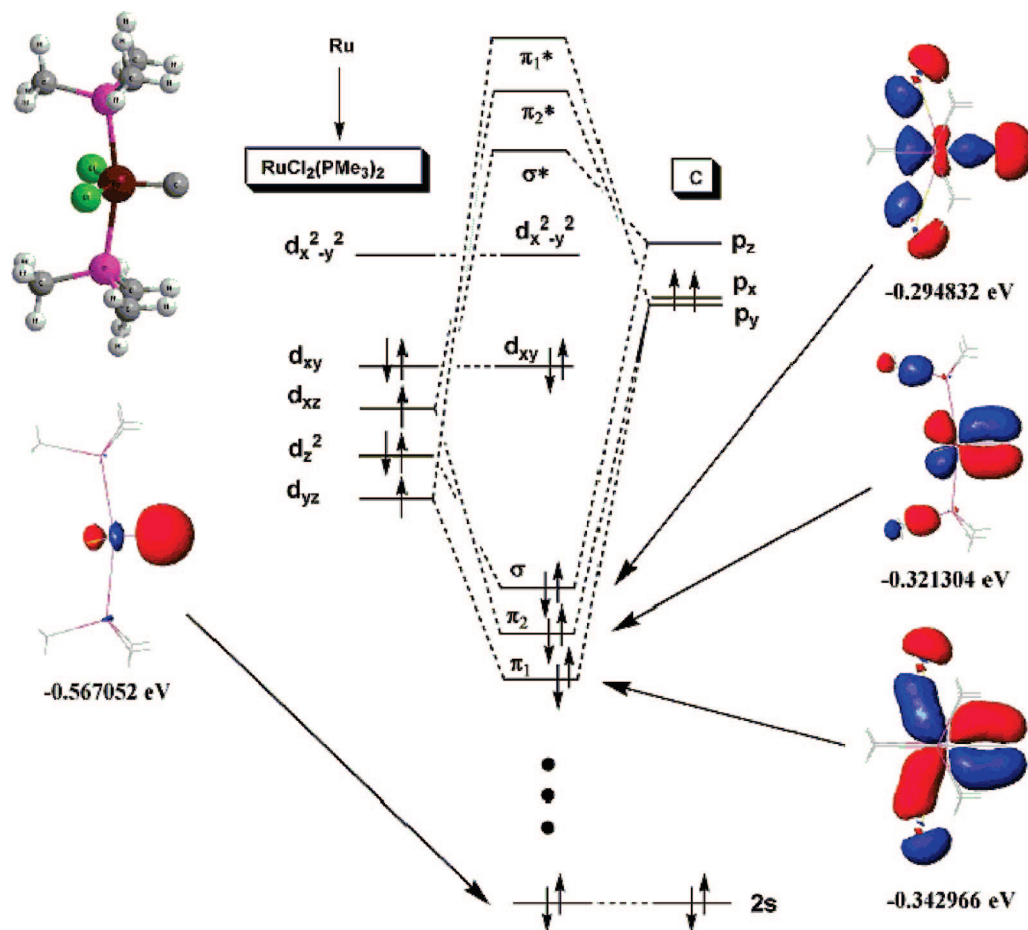


Figure 1. Orbital interaction scheme for Ru–C bonding in **Ru1M-C**.

ligands used (Chart 2). For PMe_3 and PCy_3 , two singlets and one triplet can be found as separate minima when optimizing the $\text{RuCl}_2(\text{PR}_3)_2$ geometries. This was confirmed by frequency calculations. For PMe_3 , the most stable fragment is a singlet with a “butterfly” geometry (Chart 2, Ru1 M singlet 1). The P–Ru–P angle is 100.3° ; the Cl–Ru–Cl angle is 161.5° . By comparison, a second distinct singlet structure that has a P–Ru–P angle of 176.3° and a Cl–Ru–Cl angle of 124.1° is less stable by $19.4 \text{ kcal mol}^{-1}$. A triplet species displays a nearly square-planar geometry, with identical P–Ru–P and Cl–Ru–Cl bond angles of 179.9° . This triplet species is $8.1 \text{ kcal mol}^{-1}$ higher in energy than the more stable singlet structure *with* PMe_3 ligands. These results closely parallel those reported by Krapp et al. while this paper was in revision.⁸ Also relevant are previous calculations on the structure of the $\text{Ru}(\text{PH}_3)_2\text{Cl}_2$ fragment in the context of metal $\cdots\text{H}$ agostic interactions; the accompanying discussion of the relative energies of the three minima was particularly lucid.³⁴

However, with PCy_3 ligands the most stable fragment is a square-planar triplet structure that possesses a P–Ru–P angle of 177.3° and a Cl–Ru–Cl angle of 175.3° . With these substantially bulkier ligands, the singlet structure with the smaller P–Ru–P bond angle (here, 117.4°) is $8.3 \text{ kcal mol}^{-1}$ higher in energy; the second singlet structure lies $14.3 \text{ kcal mol}^{-1}$ higher in energy than the triplet structure. Given the steric requirements of PCy_3 and the structural similarities of the triplet $\text{RuCl}_2(\text{PR}_3)_2$ fragments with the PCy_3 and PMe_3 ligands, for

Table 1. d-Orbital Energies and Electron Occupancies for the $\text{Ru}(\text{PMe}_3)_2\text{Cl}_2$ Fragment

orbital	energy (eV)	occupancy	
$4d_{x^2-y^2}$	−0.054	0	LUMO
$4d_{xy}$	−0.206	2	HOMO
$4d_{xz}$	−0.209	1	
$4d_z^2$	−0.218	2	
$4d_{yz}$	−0.233	1	

bonding analyses including bond dissociation energy determination we have chosen the square-planar triplet $\text{RuCl}_2(\text{PMe}_3)_2$ fragment as the reference geometry in the carbide-free fragment because—when the much larger PCy_3 ligands that are present in the experimental system are considered—the square-planar fragment geometry is the more stable. This choice is made in order to render the conclusions most applicable to the experimental system, in which small phosphines have never yet been found. In fact, small phosphines may not be compatible with long-lived terminal carbide complexes of Ru (*vide infra*).

Thus, the triplet spin configuration of the fragments $\text{Ru}(\text{PMe}_3)_2\text{Cl}_2$ (Table 1) and atomic C as illustrated in Figure 1 define the reference energy states of these fragments. For the Ru fragment the following orbital occupancy was assigned based upon visualization of the calculated molecular orbitals: $(4d_{yz})^1(4d_z^2)^2(4d_{xz})^1(4d_{xy})^2(4d_{x^2-y^2})^0$. This orbital occupation appears to violate the Aufbau principle in that there is a *doubly* occupied orbital (d_{xy}) at higher energy than the *singly* occupied d_{xz} orbital. Other electron configurations, including the expected alternative electron configuration $(4d_{yz})^2(4d_z^2)^2(4d_{xz})^1(4d_{xy})^1(4d_{x^2-y^2})^0$ based on the listed orbital energies of the $\text{Ru}(\text{PMe}_3)_2\text{Cl}_2$ fragment, were also examined. However, the former is found

(34) Baratta, W.; Mealli, C.; Herdtweck, E.; Ienco, A.; Mason, S. A.; Rigo, P. *J. Am. Chem. Soc.* **2004**, *126*, 5549.

Table 2. Selected Orbital Energies and Descriptions for Ru1M-C

orbital	molecular orbitals		NBO analysis		
	energy/eV	description	occupation	% Ru	% C
HOMO	-0.223125	Ru d_{xy}	1.97074	100.00	0.00
HOMO-6	-0.294832	Ru-C σ -bond	1.89073	62.23	37.74
HOMO-8	-0.321304	Ru-C π -bond (π_2)	1.93028	77.92	22.08
HOMO-10	-0.342966	Ru-C π -bond (π_1)	1.57994	65.21	34.79
HOMO-30	-0.567052	C lone pair (C 2s)	1.91864	0.00	100.00

to have the lowest energy. A similar violation of the Aufbau principle has been observed in some metal–porphyrin and metal–phthalocyanine complexes experimentally by both photoelectron and EPR spectroscopies and was also confirmed computationally.³⁵ The origin of this behavior was ascribed to the electron–electron repulsion energies.³⁵

This identified electron configuration leads directly to the formation of a triple bond to the C atom without the need for electronic excitation of either fragment. It leads to a σ -bond between the (formerly) doubly occupied Ru $4d_{z^2}$ and the (formerly) empty C $2p_z$ orbital, as well as two π -bonds, involving two electrons in Ru's $4d_{xz}$ and $4d_{yz}$ orbitals and $2e^-$ in carbon's $2p_x$ and $2p_y$ orbitals. Although consideration of the fragments suggests σ -donation from Ru to C as the origin of the Ru–C σ -bond in **Ru1M-C**, with covalent π -bonding of the two fragments accounting for the other two bonds, in the intact carbide complex **Ru1M-C** the NBO analysis is consistent with a slightly different picture: one relatively covalent σ -bond and one similar π -bond, with the second π -bond polarized strongly toward Ru (Ru–C π -donation). This discrepancy underscores the very large perturbation of the electronic structures of the fragments that occur upon formation of this very strong bond. The remaining $2e^-$ at the C atom occupy a C-based nonbonding orbital that is primarily (90%) 2s in character, which is essentially unperturbed from the free C atom. The Ru–C σ -bonding orbital is the HOMO-6, while π_1 and π_2 are HOMO-10 and HOMO-8, respectively (Table 2). Furthermore, the activation energy required to prepare the planar Ru(PMe₃)₂Cl₂ fragment for bonding to C is very small ($\Delta E^*_{\text{reorg}}$ in Table 3).

Our computational study also supports the experimental observation of the inertness of carbides **Ru1E-C** and **Ru3E-C**.⁴⁻⁷ The carbide “lone pair” is an almost pure C 2s orbital; as the HOMO-30, it is at substantially lower energy than the Ru–C σ - and π -bonds, as shown in Table 2. This accounts for the weak Brønsted and Lewis basicity observed for the carbido ligand in these complexes,⁴⁻⁷ whereas in an anionic carbide compound a less stable C 2s orbital may explain its higher reactivity.^{1,2,36}

Ru–C Bond Strengths. The dissociation energy calculated for the Ru–carbide bond (147.4 kcal mol⁻¹; see Table 3) is among the strongest reported chemical bonds that involve 4d elements. It is comparable to those of strong terminal nitride and oxide complexes of the 4d elements. For example, the experimental Mo≡N bond dissociation enthalpy (BDE) in N≡Mo(N[*t*-Bu]Ar)₃ (Ar = 3,5-C₆H₃Me₂) is 155.3 ± 3.3 kcal mol⁻¹,³⁷ and that of its oxo analogue O=Mo(N[*t*-Bu]Ar)₃ is

155.6 ± 1.6 kcal mol⁻¹,³⁸ larger than any of the E=O values tabulated by Holm over a decade ago.³⁹ Difficulties associated with preparing suitable low-coordinate precursors for atom-abstracting reactions have prevented the acquisition of *experimental* values for the metal–nitride or metal–alkylidyne triple bonds except as noted above.³⁷ In this case, DFT calculations (B3LYP/lanl2dz) on the model complex N≡Mo(NH₂)₃ predict a Mo≡N BDE of 149.8 kcal mol⁻¹,⁴⁰ in excellent agreement with the value obtained in the experimental system. In the following discussion we consider modifying the Ru carbide chemical environment as a means of activating the bond.

As seen by comparison of the BDE listed for entry 1 to those of entries 9–11 in Table 3, the Ru≡C triple bond is 60–70% stronger than a Ru=C double bond. This highlights the unexpectedly great strength of the Ru≡C bond in the carbide complex. Note that the ruthenium–carbene interactions are not unusually weak: strengths of the Ru=C bonds (in **Ru1M-CH₂**, **Ru1M-CHPh**, and **Ru1M-CHOAc**) are near the high end of bond strengths calculated for both Fischer and Schrock carbene complexes of W.⁴¹

These observations emphasize that the scarcity of terminal carbido complexes is certainly not due to weakness of the metal–carbide bond. Next, however, we consider several chemical schemes to activate the metal–carbide bond as methods for achieving new carbide complexes. The trends are shown to be consistent with the carbide bond analysis detailed above. The bond modulation depends on the orbital energies of the C atom and the frontier MOs of the Ru fragments. This can be achieved either by replacing the Ru ligands or by appending an additional group on the C atom. Functionalization of the C atom in this way generates carbyne complexes that maintain the triple bond. In Table 3 we compare the resulting carbyne complexes to their carbide analogues. According to our electronic description of Ru–C bonding, a substantial weakening of Ru–C σ -bonding upon protonation or methylation of the carbido ligand is predicted. This is associated with forced rehybridization at C that results in poorer energy matching of the C σ -symmetry orbital (formerly almost entirely $2p_z$, now a $2s-2p_z$ hybrid) with Ru $4d_{z^2}$. Below, we detail the effects of such modifications on the Ru–C bond strength.

Effect of Ancillary Ligands. We calculated Ru–C bond dissociation energies for different derivatives of the Ru complex **Ru1M-C**. The effect on the carbide bonding due to replacement of the ancillary ligands at Ru is studied by comparing model compound **Ru1M-C** (dichloride) to molecules **Ru2M-C** (dibromide), **Ru5M-C** (tetrachloride), **Ru6M-C** (tetrabromide), and **Ru7M-C** (trichloride) (defined in Chart 1). These modifications are described by the chemical formula Ru(C)(PMe₃)_{4-n}X_n for **Ru1M-C**, **Ru2M-C**, **Ru5M-C**, **Ru6M-C**, and **Ru7M-C**, where X = Cl, Br and $n = 2-4$. The calculated bond energies and bond lengths of these species are listed in Table 3.

First we study the effect of ancillary ligand electronegativity and Ru oxidation state (entries 1–5 in Table 3). Entries 1 and 3 involve more electronegative halide ligands than 2 and 4. Therefore the Ru atomic bonding orbitals in the dichloride and tetrachloride complexes **Ru1M-C** and **Ru5M-C** respectively should be lower in energy than in the corresponding dibromide and tetrabromide complexes **Ru2M-C** and **Ru6M-C**. This leads

(35) Westcott, B. L.; Gruhn, N. E.; Michelsen, L. J.; Lichtenberger, D. L. *J. Am. Chem. Soc.* **2000**, *122*, 8083.

(36) We have calculated the orbital energies of the model compound **Mo4M-C** that corresponds to Cummins' **Mo4E-C** [refs 1 and 2] and found all carbide-centered orbitals are shifted to higher energy compared to those of **Ru1M-C**, including the carbide lone pair orbital.

(37) Cherry, J. P. F.; Johnson, A. R.; Baraldo, L. M.; Tsai, Y. C.; Cummins, C. C.; Kryatov, S. V.; Rybak-Akimova, E. V.; Capps, K. B.; Hoff, C. D.; Haar, C. M.; Nolan, S. P. *J. Am. Chem. Soc.* **2001**, *123*, 7271.

(38) Johnson, A. R.; Davis, W. M.; Cummins, C. C.; Serron, S.; Nolan, S. P.; Musae, D. G.; Morokuma, K. *J. Am. Chem. Soc.* **1998**, *120*, 2071.

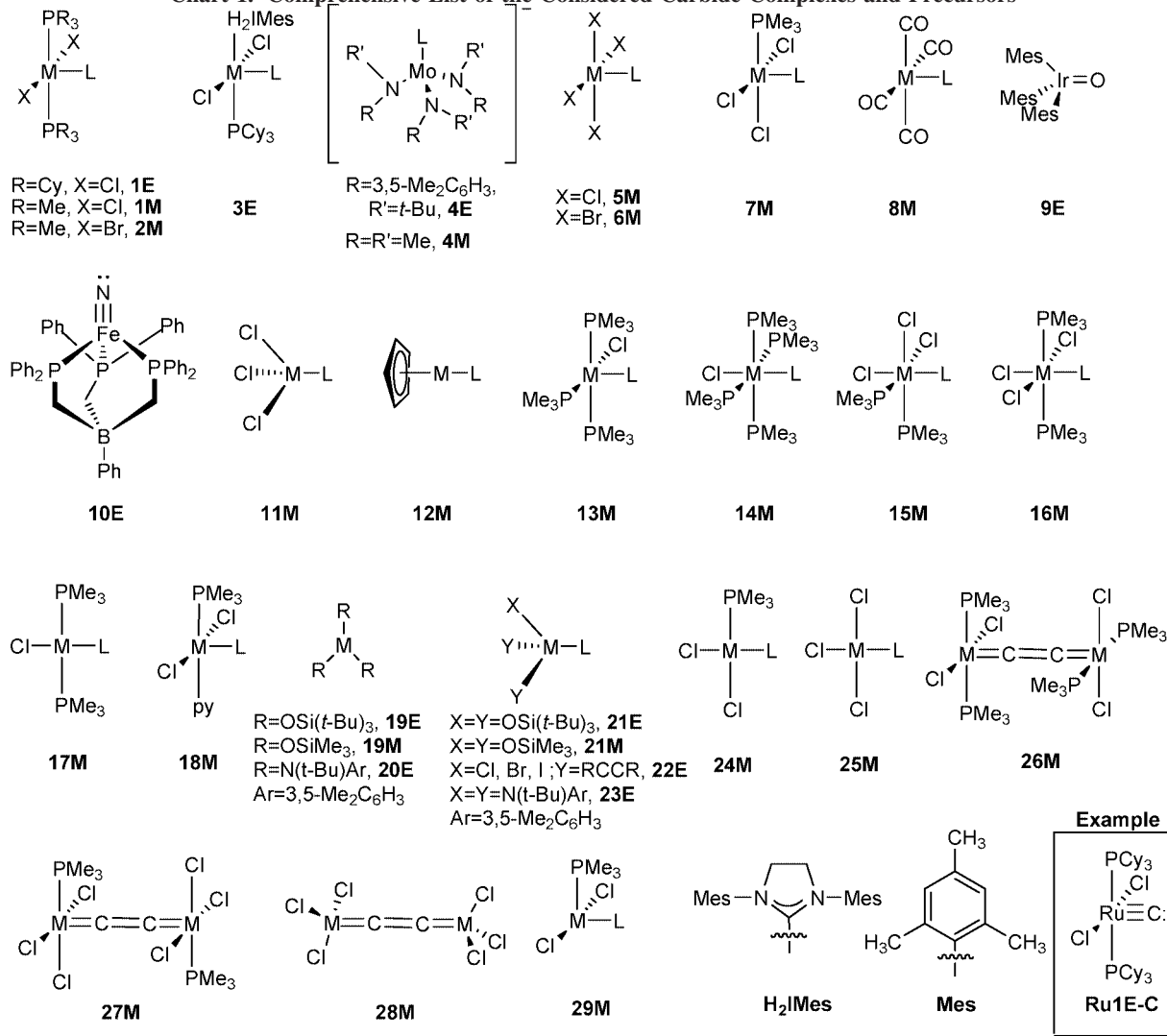
(39) Holm, R. H.; Donahue, J. P. *Polyhedron* **1993**, *12*, 571.

(40) Cui, Q.; Musae, D. G.; Svensson, M.; Sieber, S.; Morokuma, K. *J. Am. Chem. Soc.* **1995**, *117*, 12366.

(41) Vyboishchikov, S. F.; Frenking, G. *Chem.–Eur. J.* **1998**, *4*, 1428.

Table 3. Calculated Ru–C Double- and Triple-Bond Lengths and Dissociation Energies (in kcal mol⁻¹) (ground states are singlets unless otherwise specified)^a

entry	designation	Ru complex	metal fragment (multiplicity)	<i>d</i> (Ru–C) (Å)	BDE (Δ <i>E</i>)	BDE corr	Δ <i>E</i> * _{reorg}
1	Ru1M-C	Cl ₂ (PMe ₃) ₂ Ru≡C	Ru(PMe ₃) ₂ Cl ₂ (t)	1.655	147.4	143.6	0.9
2	Ru2M-C	Br ₂ (PMe ₃) ₂ Ru≡C	Ru(PMe ₃) ₂ Br ₂ (t)	1.655	143.7	140.2	3.2
3	Ru5M-C	Cl ₄ Ru≡C	RuCl ₄	1.677	79.2	76.6	37.1
4	Ru6M-C	Br ₄ Ru≡C	RuBr ₄	1.660	98.1	95.3	34.9
5	Ru7M-C	Cl ₃ (PMe ₃)Ru≡C(d)	Ru(PMe ₃)Cl ₃ (d)	1.665	109.7	106.8	21.4
6	Ru7M-CMe	Cl ₃ (PMe ₃)Ru≡CMe	Ru(PMe ₃)Cl ₃ (d)	1.674	100.0	97.5	22.7
7	Ru7M-CF	Cl ₃ (PMe ₃)Ru≡CF	Ru(PMe ₃)Cl ₃ (d)	1.693	66.2	63.6	22.7
8	Ru7M-CCl	Cl ₃ (PMe ₃)Ru≡CCl	Ru(PMe ₃)Cl ₃ (d)	1.691	73.5	71.0	23.0
9	Ru1M-CH₂	Cl ₂ (PMe ₃) ₂ Ru=CH ₂	Ru(PMe ₃) ₂ Cl ₂ (t)	1.828	93.6	89.1	6.8
10	Ru1M-CHPh	Cl ₂ (PMe ₃) ₂ Ru=CHPh	Ru(PMe ₃) ₂ Cl ₂ (t)	1.853	86.3	82.1	9.6
11	Ru1M-CHOAc	Cl ₂ (PMe ₃) ₂ Ru=CHOAc	Ru(PMe ₃) ₂ Cl ₂ (t)	1.826	85.7	82.0	6.8

^a d = doublet; t = triplet.**Chart 1.** Comprehensive List of the Considered Carbide Complexes and Precursors^a

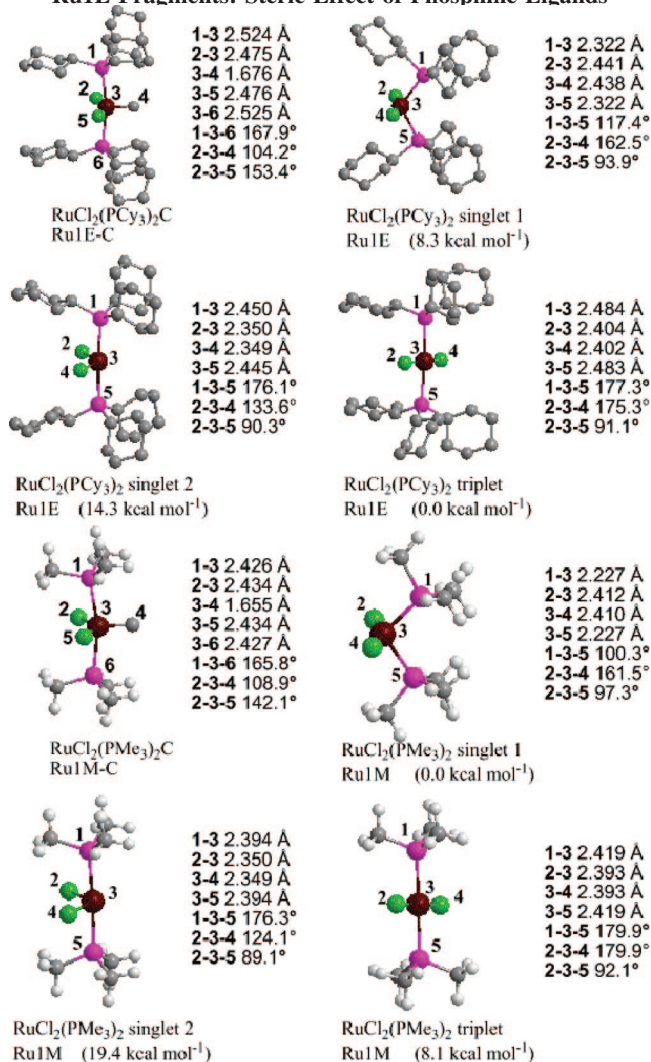
^a The notation scheme used herein is as follows. Complexes are designated according to the following scheme: (M)(LS)(type)-(UL) where (M) is the central metal, (LS) is the supporting ligand set as depicted in the Chart, (type) is either E if the compound is a known species or M if it is a computational model, and (UL) is the unique ligand of interest (if any). For example (bottom right), square-pyramidal Ru(C)(PCy₃)₂Cl₂ is denoted **Ru1E-C**.

to much more efficient bonding to C in **Ru6M-C** compared to **Ru5M-C**, although the Ru–C BDEs and bond distances of **Ru1M-C** and **Ru2M-C** are very similar. We also analyze these trends by focusing again on the Ru–C bonding orbitals.

The NBO analysis of the bonding orbitals (Table S1) indicates a similar Ru contribution to molecular orbitals for both complexes **Ru1M-C** and **Ru2M-C**: 62% for the σ-bond, 78% for π₂, and 66% for the π₁. A notable difference between these

two species is in the molecular orbital sequence. The σ-bonding molecular orbitals are HOMO–6 (for **Ru1M-C**) and HOMO–7 (for **Ru2M-C**), the π₂ are HOMO–8 (for **Ru1M-C**) and HOMO–9 (for **Ru2M-C**), and the π₁ is found at the HOMO–10 level for both Ru species.

The Ru≡C bond strengths are greatly reduced to 79 and 98 kcal mol⁻¹ upon replacement of the two phosphine ligands in **Ru1M-C** and **Ru2M-C** either by two Cl (**Ru5M-C**) or two Br

Chart 2. Comparison of Energy Minima for RuIM and RuIE Fragments: Steric Effect of Phosphine Ligands

atoms (**Ru6M-C**). As this replacement corresponds to a two-electron oxidation of the Ru center, which has a high-lying essentially nonbonding MO ($4d_{xy}$), this might have been expected to diminish the $\text{Ru}\equiv\text{C}$ BDE only slightly. Several effects can account for these observations as discussed below.

In comparing the BDEs of **Ru1M-C** and **Ru2M-C** to **Ru5M-C** and **Ru6M-C** the largest effect underlying the change in the BDEs is the relaxation energy of the RuL_4 fragment upon cleavage of the $\text{Ru}\equiv\text{C}$ bond. (Alternatively, this is the energy required to prepare the RuL_4 fragments for bonding to C, i.e., the inner sphere reorganizational energy.) The reorganization is drastic only upon the substitution of the phosphine groups as in **Ru5M-C** and **Ru6M-C** to generate RuX_4 ($X = \text{Cl}, \text{Br}$). Both **Ru5M-C** and **Ru6M-C** undergo large structural changes when the carbide ligand is removed, adopting approximately tetrahedral geometries rather than the nearly square-planar geometries of these fragments when bonded to C. In the tetrahedral geometry, both RuX_4 fragments are electronic singlets.

The relaxation energies are similar for both RuX_4 fragments and cannot account for the nearly 20 kcal mol⁻¹ difference in $\text{Ru}-\text{C}$ BDE for these two compounds. This can be explained by noting the effects of the ancillary ligands on the related orbital energy levels. The effect of the more electronegative ligand is to stabilize most Ru orbitals and particularly d_{xz} and d_{yz} . These effects are confirmed in the NBO analysis, where the decrease

in the C contribution to the bonding π_1 and π_2 bonding orbitals is strongly dependent on the ligand identity.

The effect of ancillary ligand electronegativity is seen most strikingly in the charge on the Ru atoms in **Ru1M-C**, **Ru2M-C**, **Ru5M-C**, and **Ru6M-C**, which increase in the order **Ru2M-C** < **Ru1M-C** (dihalides) < **Ru6M-C** < **Ru5M-C** (tetrahalides). The increase from **Ru6M-C** to **Ru5M-C** (tetrahalide pair) is especially dramatic (+0.203), as it is larger than the entire range spanned by **Ru2M-C**, **Ru1M-C**, and **Ru6M-C**. The effect of this increase in Ru oxidation state is also evinced in the partial charges of the C atoms in the four complexes. The carbon atom charges are more than doubled in the tetrahalide series compared to the corresponding bis(phosphine) dihalides. It is important to note that the increased oxidation state of Ru in **Ru5M-C** compared to **Ru1M-C** and the accompanying change in geometry result in a ground-state singlet for RuCl_4 , while for the $\text{RuCl}_2(\text{PMe}_3)_2$ fragment, the most stable electronic configuration is a triplet. However, the triplet→singlet relaxation of the RuCl_4 fragment (in the tetrahedral geometry) accounts for a stabilization of the RuCl_4 fragment by only 7.3 kcal mol⁻¹, making it only a minor contributor to the large 68 kcal mol⁻¹ weakening of the $\text{Ru}\equiv\text{C}$ bond observed upon going from **Ru1M-C** to **Ru5M-C**. The effects are similar but smaller for RuBr_4 .

Next we consider the effect on BDE of replacing only one phosphine ligand in **Ru1M-C** by a Cl atom. The bond dissociation energy of compound **Ru7M-C** (109.7 kcal mol⁻¹) is very close to the mean value of those of **Ru1M-C** (147.3 kcal mol⁻¹) and **Ru5M-C** (79.2 kcal mol⁻¹). This agrees well with the trend observed with regard to the energy shift in the Ru bonding orbitals when one or more ligands are substituted and its influence with respect to the electronegativity of the ligands on the $\text{Ru}-\text{C}$ bond dissociation energy. It is important to note that **Ru7M-C** is a radical species; however, as noted the HOMO has primarily Ru $4d_{xy}$ character and is approximately nonbonding ($\text{Ru}-\text{Cl} \pi^*$).

Effect of Substitution at C. The effect of varying the C environment on the strength of the $\text{Ru}\equiv\text{C}$ bond is also considered. Our interest in this point is motivated in part by the apparent instability of the protonated carbido complex (cationic methylidyne complex) $[\text{Ru}(\text{CH})(\text{PCy}_3)_2\text{Cl}_2]^+$ with respect to the isomeric phosphoniocarbene cation complex $[\text{Ru}(\text{CHPCy}_3)(\text{PCy}_3)\text{Cl}_2]^+$ as described by Piers.⁶ For example, we note that reaction of **Ru3E-C** with trifluoromethanesulfonic acid affords the corresponding phosphoniomethylidene species $[\text{Ru}(\text{CHPCy}_3)(\text{PCy}_3)\text{Cl}_2]^+$ cleanly without observable intermediates even at -90°C .¹⁷ Halocarbene complexes are also relevant in terms of 1,2-ligand migration to C as a possible mode of carbide complex decomposition (*vide infra*). The effects of varying the carbon fragment by adding groups to the C atom are studied by compounds **Ru7M-CMe**, **Ru7M-CF**, and **Ru7M-CCl**. These modifications are described by the chemical formula $\text{Ru}(\text{C}-\text{Y})(\text{PMe}_3)\text{Cl}_3$, where $\text{Y} = \text{Me}, \text{F}, \text{Cl}$. The calculated bond energies and bond lengths of these species are listed in Table 3. These calculations refer to **Ru7M-C** as a benchmark. The C atom adopts a triplet spin state with the expected $[\text{He}]2s^2 2p_y^1 2p_z^1 2p_x^0$ (choice of p orbitals is arbitrary) atomic electron configuration. The most stable spin state for the $\text{Ru}(\text{PMe}_3)\text{Cl}_3$ fragment (same fragment for complexes **Ru7M-C**, **Ru7M-CMe**, **Ru7M-CF**, and **Ru7M-CCl**) is a doublet that has the d-electron configuration $(4d_{xz})^2(4d_{yz})^2(4d_{xy})^1(4d_z)^0 - (4d_{x^2-y^2})^0$ with one unpaired electron in the Ru $4d_{xy}$ orbital. As before, this configuration assignment is based upon visualization of the calculated molecular orbitals of the $\text{Ru}(\text{PMe}_3)\text{Cl}_3$ frag-

Table 4. M≡C Bond Dissociation Energies (in kcal mol⁻¹) of Some Fe and Os Complexes

designation	metal complex	metal fragment (multiplicity)	<i>d</i> (Ru–C) (Å)	BDE (Δ <i>E</i>)	BDE corr	Δ <i>E</i> * _{reorg}
Fe1M-C	Cl ₂ (PMe ₃) ₂ Fe≡C	FeCl ₂ (PMe ₃) ₂ (t)	1.530	96.6	93.3	4.1
Fe2M-C	Br ₂ (PMe ₃) ₂ Fe≡C	FeBr ₂ (PMe ₃) ₂ (t)	1.529	98.0	94.8	2.9
Os1M-C	Cl ₂ (PMe ₃) ₂ Os≡C	OsCl ₂ (PMe ₃) ₂ (t)	1.699	167.7	163.8	1.0
Os2M-C	Br ₂ (PMe ₃) ₂ Os≡C	OsBr ₂ (PMe ₃) ₂ (t)	1.698	164.1	160.4	5.2

ment. Upon the promotion of a single electron from the highest-energy doubly occupied orbital to the LUMO in the Ru fragment, the quartet Ru fragment has a d-electron configuration of $(4d_{xz})^2(4d_{yz})^1(4d_{xy})^1(4d_{z^2})^1(4d_{x^2-y^2})^0$, which can efficiently overlap with the triplet C fragment that has the electron configuration $(2s)^2(2p_y)^1(2p_x)^1(2p_z)^0$.

These fragments interact to produce **Ru7M-C**, in which the SOMO is the Ru $4d_{xy}$ orbital. The radical character is localized on the Ru center in the $4d_{xy}$ orbital as expected since it does not interfere with orbitals required for bonding to the carbide moiety. The Ru $4d_{xy}$ orbital is an important frontier orbital. It is the HOMO in **Ru1M-C**, **Ru2M-C**, **Ru7M-CMe**, **Ru7M-CF**, and **Ru7M-CCl**, the SOMO in **Ru7M-C**, and the LUMO in **Ru5M-C** and **Ru6M-C**. These three different cases correspond to Ru oxidation states of +2, +3, and +4, respectively (if C is taken to be neutral and CR is taken to be a monocation).

Upon addition of a methyl group to the carbon atom (**Ru7M-CMe**), the electron configuration at the C atom is altered. The neutral C–Me fragment has a doublet spin state, where an electron pair occupies an sp hybrid orbital directed along the z-axis and away from the C atom of the Me group, and a single electron occupies one of the degenerate pair of orbitals. These degenerate orbitals have primarily p_x and p_y character and are destabilized slightly from those of a free C atom by interactions with filled, lower-lying C–H bonding orbitals. This agrees with the standard description for bonding in the CMe fragment.^{42,43} Analogous C–F and C–Cl fragments are also considered. In these cases, the description is similar, except that the destabilization of the C p_x/p_y-derived orbitals is due to interaction with low-lying lone pairs of the same symmetry on F and Cl, respectively.^{42,43}

The most stable geometries for all of these CX fragments have a doublet spin state that is well matched for interaction with the doublet Ru(PMe₃)Cl₃ fragment. Two effects contribute to the observed trend in Ru–C bond strengths in **Ru7M-CMe**, **Ru7M-CF**, and **Ru7M-CCl**. The energy difference between the σ and π₁*/π₂* molecular orbitals of the C–F fragment is 6.9 kcal mol⁻¹, larger than the 5.5 kcal mol⁻¹ value calculated for C–Cl and the value of 4.6 kcal mol⁻¹ found for C–Me. This correlates with the observed differences in dissociation energies (Table 3, entries 6–8). However, inductive stabilization of the C s–p_z hybrid orbital involved in Ru–C σ-bonding is also consistent with the calculated Ru–C bond weakening and likely contributes greatly to the magnitude of the observed BDE differences.

As we describe below, the inductive effect on the σ-bonding involving the C sp-hybrid orbital is also illustrated in Table S1. In contrast to the previous molecules, mixing of the C 2s AO into the C σ-symmetry orbital directed toward Ru (caused by forced rehybridization of the C atom upon appending the Y fragment) occurs; this yields Ru–C σ-bonding MOs in **Ru7M-CMe**, **Ru7M-CF**, and **Ru7M-CCl** that are polarized toward C rather than Ru. However, as in the carbide complexes the Ru–C

π-bonding MOs in **Ru7M-CMe**, **Ru7M-CF**, and **Ru7M-CCl** are polarized toward Ru. Thus, even though **Ru7M-CMe**, **Ru7M-CF**, and **Ru7M-CCl** were formally constructed from neutral fragments, the composition of the Ru–C bonding orbitals indicates that a formal bonding description involving a σ-donor [CY]⁺ fragment with π-back-donation from the accompanying [Ru(PMe₃)Cl₃][–] fragment is also an appropriate bonding description. This agrees with the customary view of bonding in Fischer carbyne complexes.^{42,43} However, it is important to note that all three Ru–C bonding MOs in each complex (**Ru7M-CMe**, **Ru7M-CF**, and **Ru7M-CCl**) have a high degree of covalency. Relaxation energies are moderately large but very similar for these three cases. Here the total relaxation energy is dominated by that of the metal fragment, as our calculations show that only a small contribution to the total relaxation energy is due to relaxation of the carbyne fragments.

In spite of the large changes in bond energies, the Ru≡C bond distances span a small range. NBO analysis (Table S1) reveals the presence of Ru≡C triple bonds in all these species. Although in general the correlation between bond length and bond strength in these compounds is poor, for those complexes that have the same d-electron configuration (HOMO, Ru $4d_{xy}$; entries 1, 2, 6–8 in Table 3) we find the expected inverse correlation between their bond length and bond strength. We next consider other factors that affect the carbide bond stability.

Effect of Metal. We now consider the effect of the metal on the carbide bond strength. At present, all but one reported neutral terminal carbido complexes contain Ru;^{4,5,7} the last is based on Os.⁴⁴ First we consider several related model complexes that contain Fe or Os in place of Ru in order to determine if only Ru favors terminal carbide formation from a thermodynamic standpoint. As already noted, the electronic structure of the square-planar Ru(PR₃)₂Cl₂ fragment appears nearly ideal for interaction with a C atom. Table 4 summarizes the effect of replacing Ru in **Ru1M-C** and **Ru2M-C** (the two complexes with the strongest Ru≡C bonds) by Fe and by Os, but retaining the same ancillary ligand sets.

From periodic trends the iron carbide is expected to have the weakest metal–carbon bond. However, as is seen, even the Fe≡C bond is predicted to be quite strong (93.3 and 94.8 kcal mol⁻¹ after ZPE correction) with these ancillary ligand sets. This is consistent with a previous study, which determined that the Fe–C bond in putative Fe(C)(CO)₄ (**Fe8M-C**) has a dissociation energy of 84.1–94.5 kcal mol⁻¹ depending on the level of theory used, and that the C atom is a very strong π-acceptor and exceptionally strong σ-donor.⁴⁵ Complex **Fe8M-C** has been proposed as an intermediate in the rather complicated reaction of Fe(CS)(CO)₄ with P(NMe₂)₃.⁴⁶ Unlike **Ru1E-C** (or its model **Ru1M-C**), the calculations predict that **Fe8M-C** should be significantly nucleophilic at C.⁴⁵

Although these BDE results suggest that the Fe≡C bond can be rather strong in some cases, these results do not address the question of the feasibility of iron–carbide formation from the

(42) Fischer, H.; Hofmann, P.; Kreissl, F. R.; Schrock, R. R.; Schubert, U.; Weiss, K. *Carbyne Complexes*; VCH Publishers: New York, 1988; p 235.

(43) Vyboishchikov, S. F.; Frenking, G. *Chem.–Eur. J.* **1998**, *4*, 1439.

(44) Stewart, M. H.; Johnson, M. J. A.; Kampf, J. W. *Organometallics* **2007**, *26*, 5102.

(45) Chen, Y.; Petz, W.; Frenking, G. *Organometallics* **2000**, *19*, 2698.

(46) Petz, W.; Weller, F. *Organometallics* **1993**, *12*, 4056.

Table 5. Bond Strength (in kcal mol⁻¹) and Bond Length Data for Additional Metal Carbides^a

entry	designation	complex	metal fragment (multiplicity)	<i>d</i> (Ru–C) (Å)	BDE (Δ <i>E</i>)	Δ <i>E</i> * _{reorg}
1	Mo8M-C	(CO) ₄ Mo≡C	Mo(CO) ₄	1.743	114.4	28.7
2	Rh7M-C	Cl ₃ (PMe ₃)Rh≡C	RhCl ₃ (PMe ₃)	1.659	98.2	22.9
3	Ir7M-C	Cl ₃ (PMe ₃)Ir≡C	IrCl ₃ (PMe ₃)	1.692	129.6	17.2
4	Mn11M-C	Cl ₃ Mn≡C	MnCl ₃ (qi)	1.555	43.8	10.2
5	Re11M-C	Cl ₃ Re≡C	ReCl ₃ (t)	1.705	156.6	0.7
6	Co12M-C	CpCo≡C	CoCp(t)	1.488	99.2	0.3
7	Rh12M-C	CpRh≡C	RhCp(t)	1.612	134.2	0.6
8	Ir12M-C	CpIr≡C	IrCp	1.647	156.1	6.4

^a t, triplet; qi, quintet.

acetoxycarbene complex as is observed for Ru.^{7,14} Previous DFT calculations indicate that the formation of **Ru1M-C** + HOAc from **Ru1M-CHOAc** is endoergic by 2.6 kcal mol⁻¹ in the gas phase.¹⁵ This reaction becomes barely favorable in CH₂Cl₂ solution,¹⁵ in agreement with the experimental observation of clean formation of **Ru1E-C** and HOAc from **Ru1E-CHOAc**.^{7,14} Although we discuss the formation of terminal carbide ligands from acetoxycarbene precursors in more detail later, we note here that we calculate that the reaction **Fe1M-CHOAc** → **Fe1M-C** + HOAc is endoergic by 13.6 kcal mol⁻¹ in the gas phase, 11 kcal mol⁻¹ less favorable than the analogous Ru case. Thus, formation of a terminal iron carbide complex in this manner is unlikely but may be feasible upon addition of a Lewis acid. Alternatively, two-electron reduction of the known iron porphyrin dihalocarbene complexes Fe(=CX₂)(TPP) (X = Cl, Br; TPP = 5,10,15,20-meso-tetraphenylporphyrinato²⁻),^{47–49} for example by the powerful reductant Ta(OSi-t-Bu₃)₃ (**Ta19E**, Chart 1),^{50,51} might reasonably be expected to afford the first terminal iron–carbide complex, although formation of a carbide-bridged diiron complex is a possibility.⁵² Fe(C)(TPP) is especially attractive as a potential C atom source in C atom transfer reactions, as the isoelectronic nitridomanganese(V) complexes with porphyrin or Schiff base ligands serve as N-donors in 2e⁻ and 3e⁻ N-transfer reactions.^{53–63}

The tabulated results for Os reveal the expected periodic trend in bond strengths due to d-orbital extent: the Os≡C bond is approximately 20 kcal mol⁻¹ (14%) stronger than corresponding Ru≡C bond. These results strongly suggest that neutral terminal carbide complexes of metals other than Ru should be accessible and that metal fragments that are isolobal to O (such as square-planar d⁶-ML₄ fragments like Ru(PMe₃)₂Cl₂) are likely candidates to exhibit strong metal–carbide bonding. Accordingly, we explored several other possible architectures for new carbide complexes.

(47) Mansuy, D. *Pure Appl. Chem.* **1980**, *52*, 681.

(48) Mansuy, D.; Lange, M.; Chottard, J. C.; Bartoli, J. F.; Chevrier, B.; Weiss, R. *Angew. Chem., Int. Ed. Engl.* **1978**, *17*, 781.

(49) Mansuy, D.; Lange, M.; Chottard, J. C.; Guerin, P.; Morliere, P.; Brault, D.; Rougee, M. *J. Chem. Soc., Chem. Commun.* **1977**, 648.

(50) LaPointe, R. E.; Wolczanski, P. T.; Mitchell, J. F. *J. Am. Chem. Soc.* **1986**, *108*, 6382.

(51) Veige, A. S.; Slaughter, L. M.; Lobkovsky, E. B.; Wolczanski, P. T.; Matsunaga, N.; Decker, S. A.; Cundari, T. R. *Inorg. Chem.* **2003**, *42*, 6204.

(52) Mansuy, D.; Lecomte, J.; Chottard, J.; Bartoli, J. *Inorg. Chem.* **1981**, *20*, 3119.

(53) Takahashi, T. Ph. D. thesis, University of Michigan, Ann Arbor, 1985.

(54) Bottomley, L. A.; Neely, F. L. *J. Am. Chem. Soc.* **1989**, *111*, 5955.

(55) Neely, F. L.; Bottomley, L. A. *Inorg. Chim. Acta* **1992**, *192*, 147.

(56) Neely, F. L.; Bottomley, L. A. *Inorg. Chem.* **1997**, *36*, 5432.

(57) Bottomley, L. A.; Neely, F. L. *Inorg. Chem.* **1997**, *36*, 5435.

(58) Woo, L. K.; Czaplá, D. J.; Goll, J. G. *Inorg. Chem.* **1990**, *29*, 3915.

(59) Woo, L. K.; Goll, J. G.; Czaplá, D. J.; Hays, J. A. *J. Am. Chem. Soc.* **1991**, *113*, 8478.

(60) Woo, L. K. *Chem. Rev.* **1993**, *93*, 1125.

(61) Chang, C. J.; Low, D. W.; Gray, H. B. *Inorg. Chem.* **1997**, *36*, 270.

(62) Birk, T.; Bendix, J. *Inorg. Chem.* **2003**, *42*, 7608.

(63) Bendix, J. *J. Am. Chem. Soc.* **2003**, *125*, 13348.

Prospects for Other Terminal Carbides. Terminal carbide complexes containing one or more CO ligands in addition to or in place of the (PMe₃)₂Cl₂ set in **Ru1M-C** and its iron homologue **Fe1M-C** have recently been discussed elsewhere.⁸ Now we consider alternative metal–carbide systems in order to enhance understanding of the metal–carbide bond and to identify reasonable synthetic targets. The metal–carbon interaction in a terminal carbido complex requires 4e⁻ from the metal in three suitably oriented orbitals in order to form a full triple bond with C, where L_nM≡C is decomposed into L_nM and C fragments, as has been done above. This description arbitrarily designates the C atom as a neutral two-electron donor, a decomposition that is not unreasonable based on the orbital interaction scheme shown in Figure 1. This also parallels the (again arbitrary) designation of the CR fragment in L_nM≡CR as CR⁺, when M is a late transition metal.^{42,43} (However, it should be noted that strict adherence to the rules for bond decomposition according to the ionic method results in formal designation of the carbide ligand as a zero-electron C²⁺ fragment.)

As discussed above, approximately *square-planar* d⁶-ML₄ fragments such as Ru(PMe₃)₂Cl₂ (Ru²⁺) [or Fe(por)] have the necessary orbital occupation of d_{z²}, d_{xz}, and d_{yz} to yield a strong triple bond to an apical C atom, where the valence d_{xy} orbital is occupied by a metal–based nonbonding electron pair. BDEs for some other representative 16-electron L₄M≡C complexes of the metals in groups 6 and 9 are included in Table 5 (entries 1–3). This table also demonstrates the influence of the fragment reorganizational energy on the calculated M≡C BDE. In particular, note that the BDE of (OC)₄Mo≡C (**Mo8M-C**) is considerably smaller than that of **Ru1M-C**. However, the sum of BDE and Δ*E** for **Mo8M-C** is 143.1 kcal mol⁻¹, in comparison to the corresponding value of 148.3 kcal mol⁻¹ in **Ru1M-C**. That Cl₃(PMe₃)Rh≡C and Cl₃(PMe₃)Ir≡C exhibit somewhat diminished BDEs compared to their isoelectronic group 8 counterparts is likely due to weaker M–C π-bonding as the metal d-orbitals become more stabilized and contracted in the later elements and as the oxidation state is increased. The effect of orbital extent is clearly seen in the greater BDEs for the heavier elements in any group: 5d > 4d > 3d. The results depicted in Table 5 highlight two other electronic configurations that also tend to favor strong metal–carbide bonding. These are tetrahedral M(C)L₃ coordination in which the electron count at M is either 12 (entries 4–5) or 16 (entries 6–8).

For optimal bonding to the C atom, as noted earlier, a metal fragment that is isolobal to O is required. The square-planar d⁶-ML₄ structure satisfies this criterion. Another structure that is isolobal to the O atom is a trigonal-planar or trigonal-pyramidal d⁴-ML₃ fragment. Entries 4 and 5 in Table 5 are two limiting cases for the group 7 elements, where the necessary +3 oxidation state is a reasonable one. In this case, the MnCl₃ fragment is seen to give rise to an especially weak Mn–C bond, even though the calculated Mn–C distance is very short (1.555 Å). This is not surprising, given the propensity of the MnCl₃

Table 6. Comparison of Corresponding 16- and 18-Electron Terminal Carbide Complexes (energies are listed in kcal mol⁻¹)

designation	complex	electron count	coord. number	<i>d</i> (Ru–C) (Å)	BDE (ΔE)	BDE corr	$\Delta E^*_{\text{reorg}}$
Re13M-C	Cl(PMe ₃) ₃ Re≡C	16	5	1.668	175.8	172.2	3.8
Re14M-C	Cl(PMe ₃) ₄ Re≡C	18	6	1.745	169.4	165.6	8.8
Rh7M-C	Cl ₃ (PMe ₃)Rh≡C	16	5	1.659	98.2	95.4	22.9
Rh15M-C	Cl ₃ (PMe ₃) ₂ Rh≡C	18	6	1.686	71.5	68.6	37.4
Rh16M-C	Cl ₃ (PMe ₃) ₂ Rh≡C	18	6	1.692	92.6	89.7	15.0

fragment to favor the high-spin quintet state. However, its 5d congener ReCl₃ has a triplet ground state and a very small reorganizational energy, and hence a large Re≡C BDE, 156.6 kcal mol⁻¹. In this last case, use of the more electron-donating NH₂ ligands in place of the Cl ligands yields an even larger BDE.⁶⁴

Entries 6–8 in Table 5 examine a perhaps less obvious fragment choice, one that is suggested by the existence of the highly unusual pseudotetrahedral complexes Re(O)(RCCR)₂X (X = Cl, Br, I) (**Re22E-O**),⁶⁵ Ir(O)(Mes)₃ (**Ir9E-O**),⁶⁶ and Fe(N)[(i-Pr)₂PCH₂]₃BPh (**Fe10E-N**).⁶⁷ These complexes are all 16-electron E≡ML₃ species; isoelectronic carbido complexes C≡ML₃ would contain 14-electron trigonal-pyramidal ML₃ fragments (where C is taken to be a neutral two-electron donor). Cyclopentadienyl complexes of the group 9 elements meet this criterion and should have very small reorganizational energies as well; entries 6–8 reveal M–C BDEs that are quite similar to those of **Ru1M-C** and its Fe and Os homologues. Here arbitrary decomposition of the metal–carbide to afford a C⁴⁻ fragment (the counterpart of formal O²⁻ and N³⁻ ligands in **Re22E-O**, **Ir9E-O**, and **Fe10E-N**) makes the analogy between the model carbide complexes **Co12M-C**, **Rh12M-C**, and **Ir12M-C** and the known oxo and nitride complexes **Re22E-O**, **Ir9E-O**, and **Fe10E-N** more readily apparent: the fragments CpM⁴⁺ (M = Co, Rh, Ir), (MeCCMe)₂XRe³⁺, Mes₃Ir²⁺, and [(i-Pr)₂PCH₂]₃-BPh)Fe³⁺ are all trigonal pyramidal d⁴-ML₃ units. Electron counts higher than d⁴ are greatly disfavored when the fourth ligand is a strong σ -donor, due to destabilization of d_{z²} in such cases, which leaves only d_{xy} and d_{x²-y²} as low-lying orbitals.⁶⁵ In contrast, when the fourth ligand is a weak σ -donor, d_{z²} is relatively stable, leading to three low-lying orbitals and hence to stability for electron counts up to d⁶.⁶⁷ Carbide appears to be an exceptionally strong σ -donor ligand.

Trans Influence in Terminal Carbido Complexes. It is important to note that to date no known complex has a ligand that occupies a coordination site trans to the carbide ligand. This correlates with a maximum expected electron count of 16e⁻ (ignoring possible π -donation from halide ligands). Our calculations that examine the effect of a trans ligand on the carbide bond strength mostly support this. As indicated in the previous section, a 16-electron count in pseudotetrahedral L₃M≡C complexes is preferred to an 18-electron count for the same reason that the 16-electron count is preferred in terminal oxo and nitrido complexes such as **Re22E-O**,⁶⁵ **Ir9E-O**,⁶⁶ and **Fe10E-N**.⁶⁷ The case of pseudooctahedral 18-electron L₅M≡C complexes versus their square-pyramidal 16-electron L₄M≡C counterparts is similar. All previously discussed carbide complexes (Tables 3–5) conform to this 16-electron count. However, calculations reported next predict the possibility for exceptions to this rule. These are listed in Table 6.

(64) Christian, G. J.; Stranger, R.; Yates, B. F. *Inorg. Chem.* **2006**, *45*, 6851.

(65) Mayer, J. M.; Thorn, D. L.; Tulip, T. H. *J. Am. Chem. Soc.* **1985**, *107*, 7454.

(66) Hay-Motherwell, R. S.; Wilkinson, G.; Hussain-Bates, B.; Hursthouse, M. B. *Polyhedron* **1993**, *12*, 2009.

(67) Betley, T. A.; Peters, J. C. *J. Am. Chem. Soc.* **2004**, *126*, 6252.

Table 7. Phosphine Dissociation Energies (in kcal mol⁻¹)

reaction	ΔH°	ΔG°
Rh16M-C → Rh7M-C + PMe₃	24.8	11.8
Rh15M-C → Rh7M-C + PMe₃	11.0	-1.8
Re14M-C → Re13M-C + PMe₃	5.5	-8.8
Re14M-CS → Re13M-CS + PMe₃	17.2	1.5

In order to probe the trans influence of the carbide ligand as well as the energetic effect of a sixth ligand on the metal–carbide bond strength, we selected two square-pyramidal 16-electron systems akin to **Ru1M-C** and examined the effect of adding an additional neutral donor ligand to generate octahedral 18-electron counterparts. Pertinent results are summarized in Table 6.

The results in Table 6 are clear and quite striking: the M–C bond is weakened when a ligand is added trans to the carbide moiety. However, even more interesting are the results of calculations to determine the energetics of single PMe₃ dissociation from these six-coordinate complexes, which is a measure of the trans influence exerted by the carbide ligand (Table 7).

The octahedral Re–carbide complex **Re14M-C** spontaneously expels one PMe₃ ligand, as does the less stable of the two six-coordinate Rh(C)(PMe₃)₂Cl₃ complexes, **Rh15M-C**. Only **Rh16M-C** is thermodynamically stable with respect to dissociation of a PMe₃ ligand. This is likely due to the high positive charge (+0.19) borne by the metal center in this complex compared to the isoelectronic complexes of Os, Ru, and Re considered above, although steric effects must also be a factor. The strong trans influence of the carbide ligand is apparent when comparing the thermodynamics for loss of phosphine from **Re14M-C** and **Re14M-CS**. In **Re14M-C**, loss of PMe₃ is favored ($\Delta G = -8.8$ kcal mol⁻¹), whereas in contrast PMe₃ loss from **Re14M-CS** is disfavored ($\Delta G = +1.5$ kcal mol⁻¹). The strong trans influence of the carbide ligand compared to the thiocarbonyl ligand is evinced in the difference between the Re–Cl bond distances in **Re14M-C** and **Re14M-CS**. **Re14M-C** has a Re–Cl bond length of 2.871 Å, a remarkable 0.239 Å longer than that calculated for the Re–Cl in bond in **Re14M-CS**. For comparison, the Re–P bonds in **Re14M-CS** are lengthened on average by only 0.01 Å and the Re–C bond is shortened by 0.082 Å (from 1.826 Å in **Re14M-CS** to 1.744 Å in **Re14M-C**). In looking at the difference between the Re–Cl bond lengths in **Re13M-C** and **Re13M-CS**, in which the Cl and carbide ligands are cis in the square-pyramidal geometry, the Re–Cl bond lengthens by only 0.026 Å from 2.499 Å in **Re13M-CS** to 2.525 Å in **Re13M-C**. These changes are accompanied by a similar lengthening of the Re–P bond by 0.03 Å on average along with a 0.102 Å shortening of the Re–C bond. Finally, note that the thiocarbonyl complexes are all stable with respect to loss of PMe₃. The dramatic lengthening of the Re–Cl bond when Cl is trans to the carbide ligand clearly demonstrates the exceptionally strong trans influence of the carbide moiety.

Scope of the S Atom Abstraction Route to Terminal Carbides. In order to further probe the reason for the weakening of the M≡C bond in the six-coordinate 18e⁻ carbide complexes

Table 8. Thermodynamics of S Atom Transfer from Thiocarbonyl Complexes^a

designation	complex	ox. st.	E.C.	C.N.	C–S BDE	ΔH for S-xfr to PMe_3	ΔG for S-xfr to PMe_3	ΔH for S-xfr to $\text{Ta}(\text{OSiMe}_3)_3$	ΔG for S-xfr to $\text{Ta}(\text{OSiMe}_3)_3$
Ru1M-CS	$\text{Ru}(\text{CS})(\text{PMe}_3)_2\text{Cl}_2$	2	16	5	94.2	19.0	20.1	–32.5	–30.4
Rh17M-CS	$\text{Rh}(\text{CS})(\text{PMe}_3)_2\text{Cl}$	1	16	4	122.3	46.6	44.5	–4.9	–5.9
Rh7M-CS	$\text{Rh}(\text{CS})(\text{PMe}_3)\text{Cl}_3$	3	16	5	107.8	32.4	33.6	–18.9	–16.6
Rh16M-CS	$\text{Rh}(\text{CS})(\text{PMe}_3)_2\text{Cl}_3$	3	18	6	123.8	48.1	48.0	–3.3	–2.4
Re13M-CS	$\text{Re}(\text{CS})(\text{PMe}_3)_3\text{Cl}$	1	16	5	101.9	26.7	27.4	–24.8	–23.0
Re14M-CS	$\text{Re}(\text{CS})(\text{PMe}_3)_4\text{Cl}$	1	18	6	113.9	38.3	37.7	–13.7	–12.7

^a ox. st. = oxidation state of metal atom; E.C. = electron count at metal center; C.N. = metal atom coordination number. ΔH_{rxn} and ΔG_{rxn} refer to the indicated reactions as drawn: either $[\text{M}]\text{-CS} + \text{PMe}_3 \rightarrow [\text{M}]\text{-C} + \text{S}=\text{PMe}_3$ or $[\text{M}]\text{-CS} + \text{Ta}(\text{OSiMe}_3)_3 \rightarrow [\text{M}]\text{-C} + \text{S}=\text{Ta}(\text{OSiMe}_3)_3$ where $[\text{M}]$ denotes some metal and its ancillary ligand set. Energies are given in kcal mol^{–1}.

in comparison to their five-coordinate $16e^-$ counterparts (Table 6), we examine sulfur atom abstraction from the corresponding rhodium thiocarbonyl complexes. Similar S atom abstraction reactions of Ru and Re thiocarbonyl complexes are compared. Experimentally, S atom abstraction from thiocarbonyl complexes has been shown to be a viable route to terminal carbide complexes of Ru and Os.^{7,44} Indeed, this route is the only route so far discovered that provides access to all extant neutral terminal carbide complexes.⁶⁸ The results reported next further support an assignment of the carbide ligand as a very strong trans influence ligand.

Carbon–sulfur bond dissociation energies (electronic) for the six compounds examined are summarized in Table 8. A thermodynamic scale for S atom transfer reactions was recently assembled.⁶⁹ The experimentally determined C–S BDE in $:\text{C}\equiv\text{S}$: itself is 170.5 ± 6.2 kcal mol^{–1}.⁷⁰ For comparison, we calculate a BDE of 163.8 kcal mol^{–1} for this process. Enthalpies and Gibbs energies of reaction with PMe_3 (forming $\text{S}=\text{PMe}_3$ as the byproduct) are also calculated, in order to account for ZPE effects.

Table 8 shows that the C–S bonds in all six thiocarbonyl complexes are significantly weakened compared to that of free CS. However, sulfur atom abstraction by PMe_3 is still energetically uphill by >19 kcal mol^{–1} in every case. Six electrons are required to cleave the triple bond in CS; two are provided by the PMe_3 reagent as is it oxidized to $\text{S}=\text{PMe}_3$. This leaves the Rh center as the source for the other four electrons needed. However, as shown in Table 8, the oxidation state of Rh is of much less importance in determining the ease of S atom abstraction than the presence or absence of a ligand trans to the incipient carbide ligand. In particular, square-planar Rh(I) (**Rh17M-CS**) and octahedral Rh(III) (**Rh16M-CS**) complexes have C–S BDEs of 122.3 and 123.8 kcal mol^{–1}, respectively. In contrast, oxidation from Rh(I) to Rh(III), coupled with removal of a neutral PMe_3 donor ligand (both of these actions should afford a metal center that is a much poorer reductant) yields a square-pyramidal thiocarbonyl complex (**Rh7M-CS**) that has a C–S BDE of only 107.8 kcal mol^{–1}. This effect must be due to an exceptionally strong trans influence of the carbide ligand compared to thiocarbonyl. We emphasize that “push-pull” π -effects cannot account for the difference because the neutral C ligand must be a much stronger π -acceptor than is CS. In fact, the “push-pull” model predicts that the carbide complex should be stabilized relative to the thiocarbonyl complex by π -donation from Cl, whereas the opposite is observed.

In this respect, it is important to note that the *only* known neutral terminal carbide complexes adopt square-pyramidal

geometries in which the carbide ligand is apical. This lack of a ligand trans to the carbide moiety underscores the strong trans influence of the carbide unit. To date there is no reagent that is known to act as a sufficiently strong S atom abstractor to yield a carbide from any of the three hypothetical Rh–CS complexes in solution.⁶⁹ However, two reagents accomplish a similar transformation in a Ru-based system. Experimentally, **Mo20E** and **Ta19E** (Chart 1) can be used to convert **Ru1E-CS** to **Ru1E-C**. **Ta19E** is known to be a stronger S-abstracting agent than **Mo20E**.⁴⁴ Although the $\text{S}=\text{Ta}$ BDE in **Ta21E-S** is not yet experimentally determined, we have calculated it to be 126.3 kcal mol^{–1} in the model complex **Ta21M-S**. As indicated, this BDE is larger than that of any of the thiocarbonyl compounds listed in Table 8: S atom abstraction by **Ta21M** is exothermic and exoergic for all the species listed in Table 8. This indicates that all of these thiocarbonyl complexes are viable starting materials for carbide formation via S atom abstraction by **Ta19E**. Thus, very reactive carbide complexes may be accessible through the use of a powerful S atom abstractor such as **Ta19E**.

Suitability of Acetoxycarbene Ligands As Precursors to Carbide Ligands. Expulsion of acetic acid from **Ru1E-CHOAc** yields **Ru1E-C** cleanly and rapidly in dichloromethane.^{7,71} In principle, decomposition of a Fischer carbene fragment to yield carbide is a relatively general method for carbide complex synthesis, although at present this route has been used to prepare only those acetoxycarbene complexes that can be prepared by olefin metathesis.^{7,44,71} In order to gain insight into the scope of this transformation, we performed additional calculations as detailed in Table 9.

As is seen in the table, expulsion of HOAc from various $\text{L}_n\text{M}=\text{CHOAc}$ complexes of the correct form to have strong M–C triple bonds is of limited utility: $16e^-$ complexes of Ru and Re can be formed spontaneously, but those of Rh cannot. Here the synthetic route of choice will be S atom abstraction, as discussed above.

It is apparent that the trans influence of the carbide ligand is much greater than that of the acetoxycarbene ligand, similar to what was seen above when thiocarbonyl ligands were compared. Comparison of the reaction energies for formation of **Rh7M-C** and **Rh16M-C** from **Rh7M-CHOAc** and **Rh16M-CHOAc**, respectively, reveals that the presence of a ligand trans to the incipient carbide makes its formation more unfavorable by over 10 kcal mol^{–1}, a difference that is very similar to the 14 kcal mol^{–1} difference found for S atom abstraction from the corresponding thiocarbonyl complexes (Table 8). Likewise, we calculate that formation of **Re13M-C** from **Re13M-CHOAc** is 6.7 kcal mol^{–1} more favorable than the corresponding formation of **Re14M-C** from **Re14M-CHOAc** (Table 9). The latter two complexes possess a sixth ligand. Although we calculate that

(68) Stewart, M. H. Ph.D. thesis, University of Michigan, Ann Arbor, 2007.

(69) Donahue, J. P. *Chem. Rev.* **2006**, *106*, 4747.

(70) Binnewies, M.; Milke, E. *Thermochemical Data of Elements and Compounds*; Wiley-VCH: Weinheim, 2002; p 928.

(71) Caskey, S. R. Ph.D. thesis, University of Michigan, Ann Arbor, 2007.

Table 9. Thermodynamics of Carbide Ligand Formation from Acetoxycarbene Ligand^a

designation	complex	electron count	ox. st.	C.N.	ΔH_{rxn}	ΔG_{rxn}
Ru1M-CHOAc	Ru(PMe ₃) ₂ Cl ₂ CHOAc	16	2	5	8.5	2.6
Rh17M-CHOAc	Rh(PMe ₃) ₂ ClCHOAc	16	1	4	31.3	23.0
Rh7M-CHOAc	Rh(PMe ₃)Cl ₃ CHOAc	16	3	5	34.2	26.3
Rh16M-CHOAc	Rh(PMe ₃) ₂ Cl ₃ CHOAc	18	3	6	43.5	36.5
Re13M-CHOAc	Re(PMe ₃) ₃ ClCHOAc	16	1	5	1.6	-3.5
Re14M-CHOAc	Re(PMe ₃) ₄ ClCHOAc	18	1	6	9.9	3.2

^a ox. st. = metal atom oxidation state; C.N. = metal atom coordination number; energies given in kcal mol⁻¹.

Table 10. Length of Ru–P Bonds and Energies (in kcal mol⁻¹) of PMe₃ Dissociation in Several Complexes

designation	Ru complex	$d(\text{Ru}-\text{P})$ (Å)	ΔH_{dissoc}	ΔE_{reorg}	$\Delta H^{\ddagger}_{\text{exch}}$
Ru1M-C	Cl ₂ (PMe ₃) ₂ Ru≡C	2.43	36.2	6.6	(unk)
Ru1M-CH₂	Cl ₂ (PMe ₃) ₂ Ru=CH ₂	2.41	24.2	3.4	(dec)*
Ru1M-CHPh	Cl ₂ (PMe ₃) ₂ Ru=CHPh	2.41	22.1	10.8	23.6 ± 0.5*
Ru1M-CHOAc	Cl ₂ (PMe ₃) ₂ Ru=CHOAc	2.41	26.5	6.4	(unk)

formation of **Re14M-C** in this way is endoergic in the gas phase, we note that formation of **Ru1E-C** by this route is favorable in CH₂Cl₂ solution, even though it is similarly unfavorable in the gas phase. Thus, the acetic-acid-expulsion route may afford even six-coordinate complexes similar to **Re14M-C**.

Phosphine Dissociation from Ru(C)(PR₃)₂Cl₂. In order to probe the feasibility of synthesis of other terminal carbide complexes from the few extant examples via ligand substitution, we focus on the phosphine dissociation reaction. At present, no exchange of the PCy₃ ligands in **Ru1E-C** or **Ru3E-C** has been reported.⁴⁻⁷ Furthermore, the basal chloride ligands in approximately square-pyramidal **Ru1E-C** and **Ru3E-C** are much less susceptible to substitution than are those in **Ru1E-CS**, **Ru1E-CHPh**, or **Ru3E-CHPh**.^{7,10-12} Finally, phosphine dissociation is a key step in olefin metathesis catalyzed by complexes **Ru1E-CHPh** and **Ru3E-CHPh**.⁷² As terminal carbide complex formation is a major decomposition pathway that must be avoided if cross-metathesis of vinyl esters is to be achieved, the effect of ligand loss on the energy of the carbene-to-carbide transformation is of critical importance. Therefore, in addition to BDE values for the Ru–C bonds, phosphine dissociation energies are also calculated. These are detailed in Table 10.

The calculated energy for dissociation of a single PMe₃ ligand from **Ru1M-CHPh** (22.1 kcal mol⁻¹) compares very well to the experimentally measured ΔH^{\ddagger} for dissociative exchange of PCy₃ in **Ru1E-CHPh** (23.6 ± 0.5 kcal mol⁻¹).⁷² The corresponding calculated value for the methyldene complex, **Ru1M-CH₂**, is 24.2 kcal mol⁻¹. Previous calculations gave similar results.⁷³⁻⁸⁴ Unfortunately, there is no experimental value for

comparison, due to decomposition of **Ru1E-CH₂** at the elevated temperature of the measurement.⁷² However, even compared to **Ru1M-CH₂**, **Ru1E-C**, and **Ru3E-C** undergo substitution of the ancillary ligands very sluggishly. In accordance with these observations, we find that the Ru–PMe₃ bond is strengthened by >35% in **Ru1M-C** compared to **Ru1M-CHOAc**, from 26.5 kcal mol⁻¹ in the latter to 36.2 kcal mol⁻¹ in the former. Note that this occurs in spite of a slight increase in the Ru–P bond length of 0.02 Å in **Ru1M-C** as compared to that in **Ru1M-CHOAc**.

We also examined dissociation of a much weaker ligand, pyridine (py), from analogues of **Ru1M-C** and **Ru1M-CHOAc**, the pyridine adducts **Ru18M-C** and **Ru18M-CHOAc**, respectively. Dissociation of py was endothermic by 28.5 kcal mol⁻¹ in **Ru18M-C**, compared to 21.6 kcal mol⁻¹ in **Ru18M-CHOAc**, a difference $\Delta(\Delta H)$ of 6.9 kcal mol⁻¹. This difference is very similar to the one noted above with the PMe₃ ligand. This has two important consequences. First, given the similar energetics the formation of the complexes Ru(≡C)(L)(py)Cl₂ (L = PCy₃, H₂IMes) (counterparts of the model complex **Ru18M-C**, but not yet known) from putative Ru(=CHOAc)(L)(py)Cl₂ (currently unknown counterpart of model complex **Ru18M-C**) is likely to be spontaneous (or close enough to thermoneutral to be promoted by Lewis acid). Second, formation of carbide from an appropriate acyloxycarbene becomes more favorable as the ancillary donor ligands become stronger. This has important implications for attempts to shut down undesired formation of carbide from Fischer carbene intermediates in attempted CM reactions of **Ru1E-CHPh** and **Ru3E-CHPh** with vinyl esters or vinyl halides. Note that results of both DFT calculations¹⁵ and experiment¹⁴ are consistent with carbide formation taking place from the bis-phosphine complex **Ru1M-CHOAc/Ru1E-CHOAc** rather than from the corresponding monophosphine complex.

The absence of observable phosphine substitution in the carbide complexes, unlike the cases of their carbene, carbonyl, and thiocarbonyl analogues, is now explicable. Both dissociative (formation of a four-coordinate 14-electron intermediate) and associative (formation of a six-coordinate 18-electron complex) pathways for such a ligand substitution reaction are energetically disfavored in the carbide complexes compared to the other complexes. Of course, the associative pathway is not a reasonable one in any event for bulky phosphines such as PCy₃. However, it should be noted that even halide exchange on Ru(C)(PCy₃)₂X₂ (X = Cl, Br), which might be expected to occur via an associative mechanism, is far less facile than in the carbene, carbonyl, and carbide analogues.^{4,5,7,10,13}

(72) Sanford, M. S.; Love, J. A.; Grubbs, R. H. *J. Am. Chem. Soc.* **2001**, *123*, 6543.

(73) Weskamp, T.; Kohl, F. J.; Heringer, W.; Gleich, D.; Herrmann, W. A. *Angew. Chem., Int. Ed.* **1999**, *38*, 2416.

(74) Vyboishchikov, S. E.; Buhl, M.; Thiel, W. *Chem.–Eur. J.* **2002**, *8*, 3962.

(75) Cavallo, L. *J. Am. Chem. Soc.* **2002**, *124*, 8965.

(76) Bernardi, F.; Bottoni, A.; Miscione, G. P. *Organometallics* **2003**, *22*, 940.

(77) Fomine, S.; Vargas, S. M.; Tlenkopatchev, M. A. *Organometallics* **2003**, *22*, 93.

(78) Fomine, S.; Ortega, J. V.; Tlenkopatchev, M. A. *J. Mol. Catal. A* **2005**, *236*, 156.

(79) Adlhart, C.; Hinderling, C.; Baumann, H.; Chen, P. *J. Am. Chem. Soc.* **2000**, *122*, 8204.

(80) Adlhart, C.; Chen, P. *Angew. Chem., Int. Ed.* **2002**, *41*, 4484.

(81) Adlhart, C.; Chen, P. *J. Am. Chem. Soc.* **2004**, *126*, 3496.

(82) Straub, B. F. *Angew. Chem., Int. Ed.* **2005**, *44*, 5974.

(83) Lippstreu, J. J.; Straub, B. F. *J. Am. Chem. Soc.* **2005**, *127*, 7444.

(84) Tsepis, A. C.; Orpen, A. G.; Harvey, J. N. *J. Chem. Soc., Dalton Trans.* **2005**, 2849.

Table 11. Energies (in kcal mol⁻¹) for Carbyne Formation via 1,2-Migration of Ancillary Ligands to C

parent designation	parent complex	rearrangement designation	rearrangement complex	ΔH	ΔG
Ru1M-C	Cl ₂ (PMe ₃) ₂ Ru≡C	Ru24M-CPMe₃	RuCl ₂ (PMe ₃)(CPMe ₃)	44.9	46.8
Ru1M-C	Cl ₂ (PMe ₃) ₂ Ru≡C	Ru17M-CCl	RuCl(PMe ₃) ₂ (CCl)	27.2	28.5
Rh7M-C	Cl ₃ (PMe ₃)Rh≡C	Rh25M-CPMe₃	RhCl ₃ (CPMe ₃)	-11.4	-10.5
Rh7M-C	Cl ₃ (PMe ₃)Rh≡C	Rh24M-CCl	RhCl ₂ (PMe ₃)(CCl)	-9.7	-8.6
Ir7M-C	Cl ₃ (PMe ₃)Ir≡C	Ir25M-CPMe₃	IrCl ₃ (CPMe ₃)	25.4	24.8
Ir7M-C	Cl ₃ (PMe ₃)Ir≡C	Ir24M-CCl	IrCl ₂ (PMe ₃)(CCl)	-1.4	-1.7

Table 12. Dimerization of Terminal Carbide Complexes via C–C Coupling

monomer designation	monomer complex	dimer designation	dimer complex	dimerization energy (SCFE in kcal mol ⁻¹)
Ru1M-C	Cl ₂ (PMe ₃) ₂ Ru≡C	Ru26M	Cl ₂ (PMe ₃) ₂ Ru=C=C=RuCl ₂ (PMe ₃) ₂ (t)	-30.7
Rh7M-C	Cl ₃ (PMe ₃)Rh≡C	Rh27M	Cl ₃ (PMe ₃)Rh=C=C=RhCl ₃ (PMe ₃) (t)	-57.3
Ir7M-C	Cl ₃ (PMe ₃)Ir≡C	Ir27M	Cl ₃ (PMe ₃)Ir=C=C=IrCl ₃ (PMe ₃)	-47.8
Re11M-C	Cl ₃ Re≡C	Re28M	Cl ₃ Re=C=C=ReCl ₃ (t)	-62.7

Other Considerations: Likely Decomposition Modes. We have outlined the factors that promote the formation of strong metal–carbide bonds. However, the strength of this interaction does not by itself determine whether a particular target complex is isolable. Decomposition reactions of the carbide species must be considered as well. We briefly consider the thermodynamic parameters for two likely decomposition modes of a terminal carbide complex.

(i) **1,2-Ligand Migration.** First, as noted by Piers, 1,2-migration of a phosphine ligand occurs readily upon protonation of the carbide ligand.^{6,17} Table 11 summarizes the energetics for the transfer of a chloride or a phosphine ligand from the metal center to the carbon atom as a function of the metal and ligand set for **Ru1M-C** and isoelectronic complexes of Rh and Ir.

In these cases, substituted carbyne complexes are the designated products. Table 11 clearly shows that this is not a concern for the neutral carbide complex of Ru, in agreement with the fact that this intramolecular rearrangement is not seen. However, square-pyramidal **Ir7M-C** may be subject to rearrangement to form the square-planar chlorocarbyne complex **Ir24M-CCl**. Its Rh homologue **Rh7M-C** is likely to undergo migration of either a Cl or a PR₃ ligand to C. In order to prevent these reactions, use of tridentate or tetradentate chelating ligands in place of the three Cl ligands or all four ancillary ligands may be required. The greater favorability of these rearrangements as the metal center becomes more oxidizing suggests that this rearrangement should be considered to reduce the metal center.

(ii) **Dimerization to Form Acetylide-Bridged Dimers.** As Table 12 indicates, dimer formation via C–C coupling to generate the L_nMCCML_n unit is always a concern. Furthermore, these results indicate that formation of terminal carbide complexes of the types proposed here by reductive cleavage of acetylide is simply not a viable synthetic route, unlike, for example, the formation of **Mo23E-N** via reaction of **Mo20E** with N₂.^{85,86}

Isolation of a terminal carbide complex must rely on blocking this decomposition mode either kinetically or thermodynamically. The use of very large ligands will permit this; dimerization reactions of even greater driving force for complexes of small ligands have been prevented by the use of suitably bulky ligand sets.^{87–89} This is the likely reason that all instances of neutral

terminal carbide complexes involve the use of at least two large ligands (not smaller than P-*i*-Pr₃). Both **Re11M-C** and **Ru1M-C** are expected to lead to MCCM units with 10e⁻ in the π-system. Accordingly, the geometrical constraints associated with dimerization of these units are qualitatively the same as those for the reductive scission of N₂ by **Mo20E**, a reaction that has been studied.^{40,90} In fact, **Re11M-C** is valence isoelectronic and isolobal to **Mo23E-N**.

Conclusions

Ten general conclusions arise from our calculations of models for known and several hypothetical carbide complexes and their precursors.

(1) The terminal metal–carbide bond can be very strong indeed. It can be comparable to strong terminal metal–nitride and metal–oxide bonds. Therefore, the dearth of terminal metal–carbide complexes is not due to inherent weakness of the metal–carbide bond, but must arise from a lack of suitable low-energy pathways for their formation or the presence of low-energy pathways for their decomposition, such as dimerization via C–C coupling or 1,2-ligand migration to C.

(2) The “parent” neutral terminal carbide complexes **Ru1M-C** and **Ru2M-C** have very strong Ru≡C triple bonds as a result of extremely good energy matching of the Ru fragment d-orbitals with the p-orbitals of an isolated C atom. Virtually no structural rearrangement is required, as indicated by the very small relaxation energies of the Ru fragments (<3.5 kcal mol⁻¹). The orbital occupancy of the Ru fragment in its electronic ground state is ideal for interaction to form three strong bonds to C.

(3) In **Ru1M-C** and **Ru2M-C** the C atom is virtually unhybridized: the Ru–C σ-bond has very little C 2s-character (the C contribution to this MO is 90% 2p). Consequently, the carbide “lone pair” orbital has 90% C 2s-character. As a result, this orbital is quite stable. This fact accounts for the very poor Bronsted and Lewis basicity of the carbide ligand in these neutral complexes.

(4) The Ru–C bonds in **Ru1M-C** and **Ru2M-C** are all polarized toward Ru. Functionalization of the C atom by appending methyl or halogen fragments to generate carbyne units forces rehybridization at C, which results in a weaker Ru–C bond that is polarized toward C.

(85) Laplaza, C. E.; Johnson, M. J. A.; Peters, J. C.; Odom, A. L.; Kim, E.; Cummins, C. C.; George, G. N.; Pickering, I. J. *J. Am. Chem. Soc.* **1996**, *118*, 8623.

(86) Laplaza, C. E.; Cummins, C. C. *Science* **1995**, *268*, 861.

(87) Cummins, C. C. *Chem. Commun.* **1998**, 1777.

(88) Cummins, C. C. *Prog. Inorg. Chem.* **1998**, *47*, 685.

(89) Hahn, J.; Landis, C. R.; Nasluzov, V. A.; Neyman, K. M.; Rosch, N. *Inorg. Chem.* **1997**, *36*, 3947.

(90) Neyman, K. M.; Nasluzov, V. A.; Hahn, J.; Landis, C. R.; Rosch, N. *Organometallics* **1997**, *16*, 995.

(5) Fe and Os analogues of **Ru1M-C** and **Ru2M-C** also possess strong $M\equiv C$ triple bonds. The $M\equiv C$ bond energies increase in the order $Fe < Ru < Os$, as expected for a homologous series of complexes in the d-block.

(6) The square-pyramidal 16-electron $L_4M\equiv C$ structure adopted by **Ru1M-C** and **Ru2M-C** is a highly favored structure even for other metals and ancillary ligands. Pseudotetrahedral 16-electron $L_3M\equiv C$ and pseudotetrahedral 12-electron $L_3M\equiv C$ structures are also particularly favored on electronic grounds for complexes of the 4d and 5d metals.

(7) The carbide ligand exerts a very strong trans influence. This is responsible for the preference for electron counts of less than 18 in most cases. This has important consequences for the choice of synthetic precursors to carbide complexes.

(8) Our calculations explain the limitations in forming carbide complexes via S atom abstraction from thiocarbonyl complexes. In geometries where there is a ligand trans to the incipient carbide, carbide formation is strongly disfavored. This is a manifestation of the exceptional trans influence of the carbide ligand.

(9) The trans influence disfavors associative ligand substitution at **Ru1M-C** (compared to homologous carbene, carbonyl, and thiocarbonyl complexes). Dissociation of an ancillary ligand from **Ru1M-C** is also much less favorable than for **Ru1M-CHR** ($R = H, Ph, OAc$). These two facts account for the observed inertness to ligand substitution in terminal carbide complexes of Ru. The latter effect also suggests that it may be possible to prevent the undesired formation of **Ru1E-C** and **Ru3E-C** from **Ru1E-CHOAc**, **Ru3E-CHOAc**, and related Fischer carbene complexes by replacing one PCy_3 ligand by a much weaker donor ligand. This would enable olefin metathesis with some substrates that are incompatible with current catalysts as a result of inactivation via carbide formation.

(10) Dimerization and ligand migration are two thermodynamically viable modes of decomposition for some terminal carbide complexes. Dimerization via C–C bond formation is thermodynamically favored in the case of small ancillary ligands for all model complexes reported here; sterically hindered ligands are likely to be needed to prevent this reaction. 1,2-Migration of a phosphine or halide ligand to C is not a concern for the $Ru(C)(PR_3)_2X_2$ complexes, but may occur in isoelectronic complexes of the group 9 metals.

In summary, we have explained the stability and inertness of terminal Ru–carbide complexes. We find that the dearth of terminal carbide complexes is not due to any inherent weakness of $M\equiv C$ bonds. Many more terminal carbide complexes can be expected in the future as new routes to their formation are found. This study serves to outline the factors that give rise to stable carbide complexes, which can be used to help in the synthesis of new carbide complexes and to tune their stability as desired.

Acknowledgment. This material is based upon work supported by the National Science Foundation under Grant No. CHE-0449459, by a Graduate Fellowship to J.B.G., and by an award from Research Corporation. We also thank the University of Michigan and the Camille and Henry Dreyfus Foundation for support.

Supporting Information Available: Calculation details; NBO analysis for Ru–carbene, –carbyne, –carbide complexes. This material is available free of charge via the Internet at <http://pubs.acs.org>

OM0702072